Research Article | Vol. 27, No. 9 | 29 Apr 2019 | OPTICS EXPRESS 12806
Optics EXPRESS

Performance-enhanced gigabit/s MIMO-OFDM visible light communications using CSI-free/dependent precoding techniques

YANG HONG,[1,3] LIAN-KUAN CHEN,[1] AND JIAN ZHAO[2,*]

[1]*Department of Information Engineering, The Chinese University of Hong Kong, Hong Kong, China*
[2]*South China University of Technology, Guangzhou, China*
[3]*Currently with Optoelectronics Research Centre, University of Southampton, Southampton, United Kingdom*
**zhaojian@scut.edu.cn*

Abstract: In this paper, we propose two digital signal processing (DSP) techniques, the orthogonal circulant matrix transform (OCT) technique and the singular value decomposition (SVD)-based adaptive loading, to reduce the bit error rate (BER) of multiple-input-multiple-output orthogonal frequency division multiplexing (MIMO-OFDM)-based visible light communication (VLC) systems, without and with using the channel state information (CSI), respectively. A gigabit/s 2 × 2 MIMO-OFDM VLC system under ~100-MHz system bandwidth, with both symmetrical and asymmetrical MIMO setups, is demonstrated. It is shown that both techniques can attain outstanding BER reduction regardless of the transceivers' geometrical distributions. The SVD-based adaptive loading exhibits the best performance but requires the CSI. The OCT technique can achieve suboptimal performance without the needs of CSI. In both the 1.6-Gbit/s symmetrical MIMO setup and the 1.2-Gbit/s asymmetrical setup, we achieved more than one and two orders of magnitude reductions in the BER by using the OCT technique and the SVD-based adaptive loading, respectively.

1. Introduction

With the substantial increase in the number of multimedia-capable and Internet-connected mobile devices, e.g., smartphones and tablets, the explosion of wireless data traffic has been witnessed in recent years [1]. The conventional radio frequency (RF) communications, however, suffer from various issues, such as overcrowded spectrum and electromagnetic interference. It is essential to develop an alternative or supplementary wireless communication technology, so as to satisfy the increasing traffic demand. Recently, visible light communication (VLC) is rapidly emerging as an attractive solution for future high-speed wireless access. The dual functionality offered by VLC, i.e., the primary illumination function and the high-rate communication function, has enabled a wide range of applications for both indoor and outdoor scenarios [2]. Although 10-Gbit/s data rates were demonstrated in VLC, expensive and/or specially designed devices, e.g. injection-locked and impedance-matched lasers were required to enhance the system bandwidth beyond 1 GHz [3–5]. Predominantly, the main challenge for VLC, using the off-the-shelf components, to provide high-speed data communication is the severe frequency roll-off, induced by the limited system bandwidth [6]. To overcome the limitation, prior works including digital signal processing (DSP) [6–9] and analog circuit based equalization [10] have been reported, most of which lay emphasis on single-input and single-output (SISO) VLC systems.

Multiple-input multiple-output (MIMO) technique, on the other hand, offers the potential to achieve a linear capacity enhancement with the increase in the number of transceivers via parallel transmissions. It is particularly attractive for VLC systems since most likely more than one lighting devices are employed to provide sufficient and uniform illumination [11]. In addition, by using the MIMO technique, the coverage of VLC systems can further be

#360845 https://doi.org/10.1364/OE.27.012806
Journal © 2019 Received 26 Feb 2019; revised 7 Apr 2019; accepted 7 Apr 2019; published 22 Apr 2019

Optics EXPRESS

enlarged. Most of prior investigations on the performance of MIMO VLC were based on numerical simulations [12–14]. Experimental demonstrations showed that it was possible to realize gigabit/s VLC transmissions using 4 × 9 MIMO orthogonal frequency division multiplexing (OFDM) [15]. The frequency- and time-domain averaging approaches were proposed to further improve the system performance [16]. The analog circuits based equalization was also introduced to MIMO VLC in [17]. Extended from the SISO systems, the key issues to enhance the capacity of MIMO VLC systems using low-cost devices are not only to relax the effect of limited system bandwidth but also to achieve joint performance optimization over MIMO subchannels.

In this paper, we propose and experimentally investigate two DSP-enabled techniques, orthogonal circulant matrix transform (OCT) technique and the singular value decomposition (SVD) based adaptive loading, for MIMO-OFDM systems without and with the channel state information (CSI). Both symmetrical and asymmetrical MIMO setups are considered. It is shown that both techniques can greatly improve the performance in both setups. The SVD-based adaptive loading offers the best performance, while the OCT technique provides substantial BER reduction without the needs of the CSI.

2. Principles of the proposed schemes

2.1 The OCT technique

Figure 1 shows the block diagram of the MIMO-OFDM based VLC system. Without loss of generality, we consider a MIMO-OFDM VLC system with n_T transmitters (Txs), n_R receivers (Rxs), and K data subcarriers. We use the term 'subchannel' to denote the equivalent channel of the MIMO VLC system after either zero-forcing (ZF) detection or SVD decoding.

Generally, VLC systems use low-cost low-bandwidth devices to achieve high data rate. This results in lower SNR conditions at the high-frequency subcarriers of the recovered signal. The OCT technique was originally proposed for the SISO VLC system to spread the degradation of high-frequency subcarriers over all subcarriers, so that the overall performance could be improved [9]. Different from the SISO case, in this work we propose the OCT technique for MIMO VLC to address the performance disparity between not only different subcarriers within each transceiver but also different transceivers, wherein the latter depends on the geometrical distributions of transceivers. We consider two implementations: The first implementation, termed as the individual OCT technique, employs the OCT technique at each transmitter, i.e., multiple OCT precoding operations are carried out in parallel at the transmitters. This implementation is a direct extension of the SISO case and spreads the SNR degradation only within each subchannel. It will be shown that this implementation is only beneficial to the symmetrical setup in MIMO VLC. The second implementation, termed as the joint OCT technique, considers all subcarriers in all subchannels. This technique can improve the performance regardless of the geometrical positions of transceivers. Detailed implementations will be given in the following.

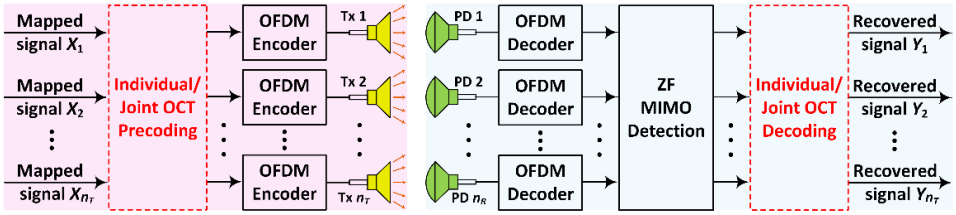

Fig. 1. Block diagram of the MIMO-OFDM VLC system. The case with the dashed blocks denotes the MIMO-OFDM system using the individual/joint OCT technique.

In the individual OCT technique, the data subcarriers in each subchannel are spread by an orthogonal circulant (OC) matrix $\boldsymbol{F}$, i.e., $\bar{\boldsymbol{X}} = [\bar{\boldsymbol{X}}_1; \bar{\boldsymbol{X}}_2; \ldots; \bar{\boldsymbol{X}}_{n_T}]^{\mathrm{T}} = [\boldsymbol{F}\cdot\boldsymbol{X}_1; \boldsymbol{F}\cdot\boldsymbol{X}_2; \ldots; \boldsymbol{F}\cdot\boldsymbol{X}n_T]^{\mathrm{T}}$,

where $\boldsymbol{X}_i = [X_i(1), X_i(2), \ldots, X_i(K)]^{\mathrm{T}}$ denotes the K subcarriers of the OFDM signal from the i-th transmitter ($1 \le i \le n_T$). The OC matrix $\boldsymbol{F}$ is channel-independent and can be expressed as

$$[\boldsymbol{F}]_{K\times K} = \frac{1}{\sqrt{K}}\begin{bmatrix} f_1 & f_2 & \cdots & f_K \\ f_K & f_1 & \cdots & f_{K-1} \\ \cdots & \cdots & \cdots & \cdots \\ f_2 & f_3 & \cdots & f_1 \end{bmatrix}, \tag{1}$$

In order to enable $\boldsymbol{F}$ to be orthogonal, the sequence $[f_1\ f_2\ \ldots\ f_K]$ should be uncorrelated with any of its delay. The Zadoff-Chu sequence [18] is the one that can meet this requirement. The numbers of multipliers and adders for each OCT operation are $K\log_2 K - 3K + 4$ and $3K\log_2 K - 3K + 4$, respectively [19]. The pre-coded signals are then transmitted and MIMO-detected in the same way as in the conventional MIMO-OFDM VLC system. After zero-forcing (ZF) detection, different subcarriers of each recovered subchannel, $[Y_{ZF,i}(1), Y_{ZF,i}(2), \ldots, Y_{ZF,i}(K)]$, are decoded by multiplying the inverse matrix of $\boldsymbol{F}$. We assume $SNR_i(k)$ and $SNR_{indv,i}(k)$ are the SNR of the k-th subcarrier of the i-th subchannel ($1 \le i \le n_T$) before and after the de-spreading. Because the constructed OC matrix is orthogonal, a uniform SNR can be achieved for different subcarriers within each subchannel after de-spreading, which can be derived as:

$$\begin{cases} \boldsymbol{SNR}_{indv,i} = \left[SNR_{indv,i}(1), SNR_{indv,i}(2), \ldots, SNR_{indv,i}(K) \right] \\ SNR_{indv,i}(1) = SNR_{indv,i}(2) = \cdots = SNR_{indv,i}(K) = \dfrac{K}{\sum_{k=1}^{K} \dfrac{1}{SNR_i(k)}} \end{cases} \tag{2}$$

It is clear in Eq. (2) that by using the individual OCT technique, within each MIMO subchannel, a uniform SNR profile equal to the harmonic mean of the original SNRs is achieved. In this way, the severe frequency roll-off issue can be tackled, resulting in significant performance improvement, as will be shown in the experiments.

The main problem of the above design is that different subchannels still exhibit performance disparity due to different geometrical positions of transceivers, causing degradation of overall performance. Therefore, we then consider the joint OCT technique, which is given by $\tilde{\boldsymbol{X}} = [\tilde{\boldsymbol{X}}_1, \tilde{\boldsymbol{X}}_2, \ldots, \tilde{\boldsymbol{X}}_{n_T}]^{\mathrm{T}} = \boldsymbol{F}'\cdot[\boldsymbol{X}_1; \boldsymbol{X}_2; \ldots; \boldsymbol{X}n_T]^{\mathrm{T}}$, where $\boldsymbol{F}'$ is the OC matrix for the joint OCT technique and is given by

$$[\boldsymbol{F}']_{(K\cdot n_T)\times(K\cdot n_T)} = \frac{1}{\sqrt{K\cdot n_T}}\begin{bmatrix} f_1' & f_2' & \cdots & f_{K\cdot n_T}' \\ f_{K\cdot n_T}' & f_1' & \cdots & f_{K\cdot n_T-1}' \\ \cdots & \cdots & \cdots & \cdots \\ f_2' & f_3' & \cdots & f_1' \end{bmatrix}, \tag{3}$$

where f_l' ($1 \le l \le K\cdot n_T$) is the corresponding element of the ZC sequence with a length of $K\cdot n_T$. The implementation of Eq. (3) is more complicated than that of Eq. (1). The numbers of required multipliers and adders for implementing the joint OCT technique are $(K\cdot n_T)\log_2(K\cdot n_T) - 3(K\cdot n_T) + 4$ and $3(K\cdot n_T)\log_2(K\cdot n_T) - 3(K\cdot n_T) + 4$, respectively. In contrast, the individual OCT technique totally only needs $n_T \times (K\log_2 K - 3K + 4)$ multipliers and $n_T \times (3K\log_2 K - 3K + 4)$ adders. Fortunately, we can simplify the implementation of the joint technique by using two steps: 1) we precode different subchannels of each subcarrier; 2) different subcarriers of each subchannel are then precoded. The complexity using this process is $n_T \times (K\log_2 K - 3K + 4) + K \times (n_T\log_2 n_T - 3n_T + 4)$ multipliers and $n_T \times (3K\log_2 K - 3K + 4) + K \times (3n_T\log_2 n_T - 3n_T + 4)$ adders, which is lower than that using Eq. (3). Figure 2 shows the comparison of the implementation complexity of the three designs in a MIMO system with 8

Optics EXPRESS

Txs. It is seen that the complexity of all designs increases as the number of data subcarriers increases. The simplified joint OCT technique exhibits only slightly higher complexity, especially for the number of multipliers, than the individual OCT technique, while it can be applied to any MIMO setup regardless of the geometrical distributions of the transceivers. By the joint OCT technique, the SNRs of the subcarriers in all the MIMO subchannels can be equalized to the same level:

$$\begin{cases} \boldsymbol{SNR}_{joint,1} = \boldsymbol{SNR}_{joint,2} = \cdots = \boldsymbol{SNR}_{joint,n_T} \\ \boldsymbol{SNR}_{joint,i} = \left[SNR_{joint,i}(1), SNR_{joint,i}(2), ..., SNR_{joint,i}(K) \right] \\ SNR_{joint,i}(1) = SNR_{joint,i}(2) = \cdots = SNR_{joint,i}(K) = \dfrac{K \cdot n_T}{\sum_{i=1}^{n_T} \sum_{k=1}^{K} \dfrac{1}{SNR_i(k)}} \end{cases} \tag{4}$$

By comparing Eqs. (2) and (4), it is found that the joint OCT technique can realize a uniform SNR profile over subcarriers for all MIMO subchannels, whereas the individual OCT technique can only realize uniform SNRs within each MIMO subchannel. Generally, it is expected that the performances of the two designs should be similar when the SNR conditions of the subchannels are comparable. A typical scenario for this case is that the MIMO system has a symmetrical system configuration, namely, the transmitters and the receivers are geometrically symmetrical. However, when the sub-channels' SNR conditions differ with each other significantly, e.g., in an asymmetrical MIMO setup, the joint OCT technique should achieve better performance than that of the individual OCT technique. This is due to the fact that the average BER performance of the MIMO system is mainly limited by the subchannel with the worst SNR condition.

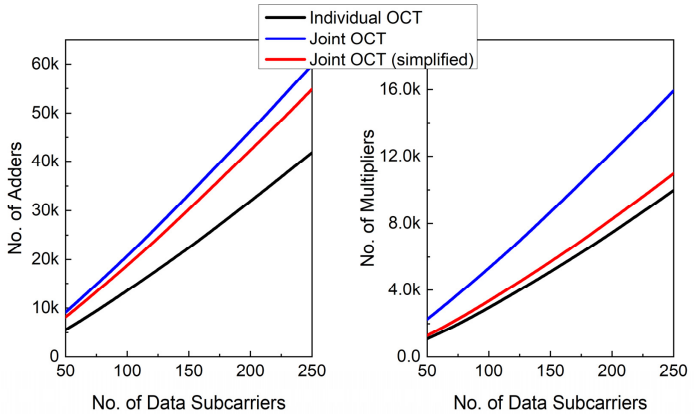

Fig. 2. Complexity of different OCT designs.

Finally, it is worth noting that the OCT techniques have similar complexity as that of the DFT precoding but they exhibit superior tolerance to inter-symbol interference as has been verified in the SISO case [9]. We note that some other precoding schemes were proposed in the literature to reduce the implementation complexity of the overall precoded system [20]. However, they assume that the number of data subcarriers and the IDFT size are the same, and so cannot be applied to the VLC systems where Hermitian extension is required between the OFDM precoding and the IDFT.

2.2 SVD-based adaptive loading

While the OCT technique exhibits the advantage of CSI-free characteristic, its performance is sub-optimal, as this technique does not fully exploit the channel information. In SISO/MIMO

Optics EXPRESS

OFDM systems, adaptive loading [21,22] can be used to maximize the capacity according to the channel response if this information is available. In this sub-section, we will investigate the SVD-based adaptive loading to utilize the CSI for the MIMO VLC system. The estimated channel matrix on the k-th subcarrier of the MIMO-OFDM VLC system, $\boldsymbol{H}(k)$, can be decomposed to:

$$\boldsymbol{H}(k) = \boldsymbol{U}(k) \cdot \boldsymbol{D}(k) \cdot \boldsymbol{V}^{\mathrm{H}}(k), \tag{5}$$

where $\boldsymbol{U}(k)$ and $\boldsymbol{V}(k)$ are $N_R \times N_R$ and $N_T \times N_T$ unitary matrices, respectively; $(\cdot)^{\mathrm{H}}$ denotes the conjugate transpose operation; and $\boldsymbol{D}(k)$ is an $N_R \times N_T$ diagonal matrix with its nonnegative diagonal entries $\lambda_{m,k}$ being the singular values of $\boldsymbol{H}(k)$, where $m = 1, 2, \ldots, M$ and $M = min\ (n_T, n_R)$. Subsequently, the unitary matrix $\boldsymbol{V}(k)$ is used to pre-code the originally transmitted signal vector $\boldsymbol{X}(k) = [X_1(k), X_2(k), \ldots, X_{NT}(k)]^{\mathrm{T}}$ at the transmitters, as shown in Fig. 3. The pre-coded signal vector after the SVD at the transmitters can be expressed as:

$$\boldsymbol{X}'(k) = \boldsymbol{V}(k) \cdot \boldsymbol{X}(k). \tag{6}$$

At the receivers, the unitary matrix $\boldsymbol{U}^{\mathrm{H}}(k)$ is used for the corresponding SVD decoding in the frequency domain, i.e.,

$$\boldsymbol{Y}'(k) = \boldsymbol{U}^{\mathrm{H}}(k) \cdot \left\{ \boldsymbol{H}(k) \cdot \boldsymbol{X}'(k) + \boldsymbol{N}(k) \right\} = \boldsymbol{D}(k) \cdot \boldsymbol{X}(k) + \boldsymbol{N}'(k). \tag{7}$$

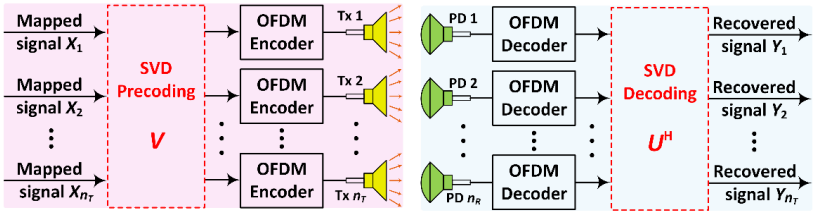

Fig. 3. Block diagram of the SVD-based adaptive loading.

Due to the diagonal property of matrix $\boldsymbol{D}(k)$, the original transmitted signal vector $\boldsymbol{X}(k)$ can be recovered without inter/intra subchannel interference, and the corresponding equivalent gains on the k-th subcarrier are represented by the diagonal entries of the matrix $\boldsymbol{D}(k)$. We assume the equivalent gains of the m-th subchannel at the k-th subcarrier are denoted by $\lambda_{m,k}$. Since the K data subcarriers in each OFDM symbol are orthogonal, the MIMO-OFDM VLC system can be decomposed into $M \times K$ orthogonal components with the equivalent gains being $[\lambda_{1,1}, \lambda_{1,2}, \ldots, \lambda_{1,K}; \lambda_{2,1}, \lambda_{2,2}, \ldots, \lambda_{2,K}; \ldots ; \lambda_{M,1}, \lambda_{M,2}, \ldots, \lambda_{M,K}]$. After obtaining the equivalent gains of the decomposed MIMO-OFDM channel, they can be used for adaptive bit and power loading in a similar manner as in the SISO case [22], except that the total bits and power used for $M \times K$ subcarriers' loading are the corresponding aggregate values of the overall system. In this way, the bits and power resources of all subchannels can be jointly optimized, ensuring both inter- and intra-subchannel optimizations. Note that the implementation of adaptive bit- and power-loading has two different ways depending on the objectives. The first approach is to maximize the achievable data rate for a certain BER threshold. The other way is to minimize the BER under a certain data rate. For fair comparison of the schemes studied in this work, we maintain the same data rate for all schemes and evaluate the corresponding BER performance.

2.3 Implementation comparisons

To help understand the investigated DSP schemes, we summarize the implementation comparisons in Table 1. It is clear that the proposed OCT techniques are independent of the MIMO VLC channel. Furthermore, only linear transformations are required and the corresponding complexity analysis has been presented in Fig. 2. In contrast, to realize the

Optics EXPRESS

SVD-based adaptive loading, pilot MIMO-OFDM transmission is firstly required to obtain the CSI. Based on the estimated MIMO channel matrix over K subcarriers, SVD is performed on each subcarrier to obtain the equivalent gains, which are subsequently used for adaptive bit and power loading. Following the pilot transmission, the SVD precoding and decoding, as described in Eqs. (6) and (7), are implemented in data transmissions to realize the SVD-based adaptive MIMO-OFDM. Apparently, the realization of the SVD-based adaptive loading relies on the prior knowledge of CSI, and its latency is much higher than that of the OCT techniques.

Table 1. Implementation comparisons of different DSP schemes in $n_T \times n_R$ MIMO-OFDM VLC

Scheme	Additional processing at Txs	Additional processing at Rxs
Conventional MIMO-OFDM	Nil	Nil
Individual OCT technique	n_T ($K \times K$)-linear transformations	n_T ($K \times K$)-linear transformations
Joint OCT technique	one ($n_T K \times n_T K$)-linear transformation	one ($n_T K \times n_T K$)-linear transformation
Joint OCT technique (simplified)	K ($n_T \times n_T$)-linear transformations n_T ($K \times K$)-linear transformations	K ($n_T \times n_T$)-linear transformations n_T ($K \times K$)-linear transformations
SVD-based loading	pilot transmission & CSI estimation K ($n_R \times n_T$)-SVD operations adaptive bit and power loading K ($n_T \times n_T$)-linear transformations	K ($n_R \times n_R$)-linear transformations

3. Experimental setup

The experimental setup of a 2 × 2 MIMO-OFDM VLC system is illustrated in Fig. 4. We investigated two scenarios: in scenario 1, the locations of Txs and Rxs were geometrically symmetrical, which resulted in similar SNR conditions between subchannels. In contrast, there was a 5-cm offset between the centers of Txs and Rxs in scenarios 2, leading to a geometrically asymmetrical MIMO setup.

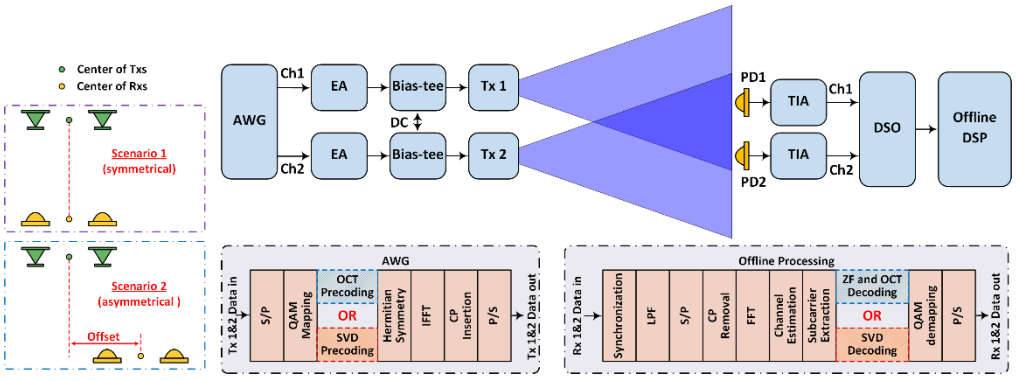

Fig. 4. Configurations of the two MIMO-VLC scenario (left), and the experimental setup (right).

At the transmitters, the offline generated signals were fed into an arbitrary waveform generator (AWG). Two outputs of the AWG were firstly amplified by two electrical amplifiers (EAs) and were then used to drive two blue lasers. The beam divergence of the LDs was $\theta_{\parallel} \times \theta_{\perp} = 11deg \times 25deg$, which ensured a relatively broad radiation and thus a wide coverage. It is worth noting that although blue lasers were used in the experiments, the proposed techniques could be readily adopted in LED-based MIMO VLC systems for performance enhancements. After 1-m free-space transmission, the signals were detected by two PIN photodiodes. For each receiving branch, the detected signal was amplified by a trans-impedance amplifier (TIA) and then recorded by a real-time digital storage oscilloscope (DSO) for further offline DSP. The system had a 3-dB bandwidth of ~100 MHz bandwidth,

Optics EXPRESS

which was mainly limited by the PIN PD's bandwidth and the impedance mismatching of the receiver module. In the experiments, the block size of FFT was 256, and 127 of that were modulated with data in each OFDM symbol. The distances between the two Txs and two Rxs were 5 cm and 4 cm, respectively.

4. Experimental results and discussions

4.1 The conventional MIMO-OFDM VLC

We first investigate the performance of the conventional MIMO-OFDM VLC system as a benchmark. Figure 5 shows the SNR profiles of the conventional MIMO-OFDM VLC system with the symmetrical (scenario 1) and asymmetrical (scenario 2) setups. The length of cyclic prefix (CP) is 1/16 of one OFDM symbol and the sampling rate of AWG is 400 MS/s. The quadrature amplitude modulation (QAM) formats for scenarios 1 and 2 are 16QAM and 8QAM respectively, which corresponded to the data rates of 1.6 Gbit/s and 1.2 Gbit/s, respectively.

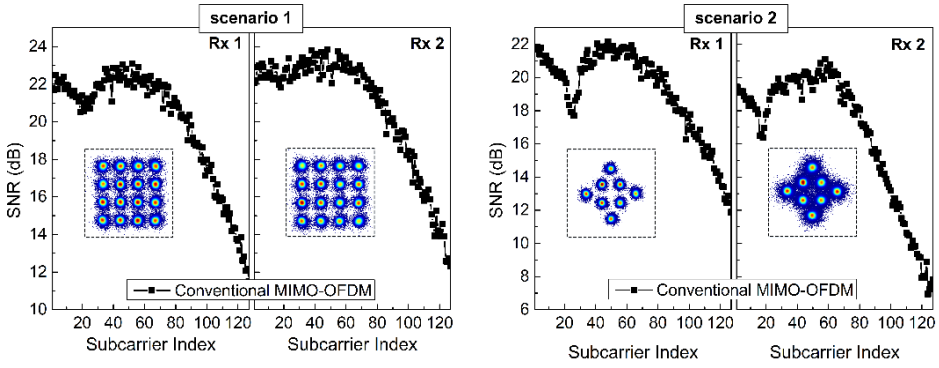

Fig. 5. The SNR profiles of the conventional MIMO-OFDM VLC system in two scenarios. Insets: the corresponding constellation diagrams.

From Fig. 5, it is seen that the system suffers from severe bandwidth limitation for both scenarios. The SNR fluctuations over subcarriers are more than 10 dB. In Fig. 5(a), the two Rxs exhibit similar SNR performance in the symmetrical MIMO setup. The BERs of Rx 1 and Rx 2 are measured to be 2.35×10^{-3} and 1.64×10^{-3}, respectively. In scenario 2, due to the asymmetrical MIMO setup, Rx 1 exhibits much higher SNRs due to its higher received signal intensity. The BERs of the two Rxs are 1.34×10^{-4} and 6.95×10^{-3}, respectively.

4.2 The OCT technique

Figure 6 shows the SNR profiles for the individual and joint OCT techniques in the symmetric and asymmetric scenarios. It is seen that uniform SNR profiles are achieved over data subcarriers within each subchannels for both individual and joint OCT. In Fig. 6(a), because the MIMO setup is symmetric, when the individual OCT technique is applied, only a slight SNR difference is observed between the two Rxs. The BERs of the two Rxs are measured to be 9.29×10^{-5} and 2.28×10^{-5}, respectively. The SNR profiles of the two Rxs are nearly identical by using the joint OCT technique. Their corresponding BERs are 5.35×10^{-5} and 4.17×10^{-5}, respectively.

In contrast, for scenario 2, when the individual OCT technique is applied, the SNR difference between Rxs is significant, although the SNR profile within each subchannel is still flat. The BERs are less than 10^{-6} for Rx 1, and 9.18×10^{-4} for Rx 2, respectively. On the other hand, the joint OCT technique achieves a uniform SNR profile over all the Rxs, and similar BERs, 4.72×10^{-5} and 5.98×10^{-5}, can be achieved for the two Rxs, respectively.

Optics EXPRESS

These observations match the theoretical analysis in Section 2. It is also derived that the joint OCT technique exhibits a smaller overall BER than that individual OCT technique.

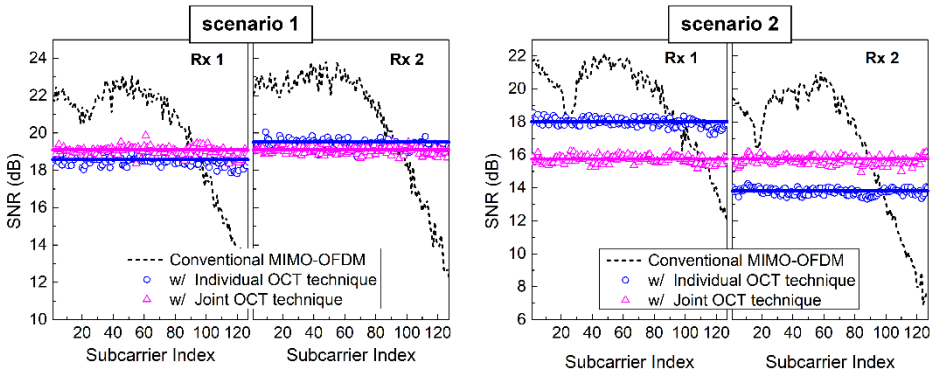

Fig. 6. Comparisons of the SNR profiles of the MIMO-OFDM VLC system using the individual/joint OCT technique in the symmetrical and asymmetrical scenarios. Solid lines denote the theoretical SNR levels calculated by Eqs. (2) and (4).

4.3 The SVD-based adaptive loading

In this sub-section, we investigate the performance of the proposed SVD-based adaptive loading technique. For fair comparisons, the transmission conditions are the same as those in Subsections 4.1 and 4.2, namely, the data rates are also 1.6 Gbit/s and 1.2 Gbit/s for the symmetrical and asymmetrical setups, respectively.

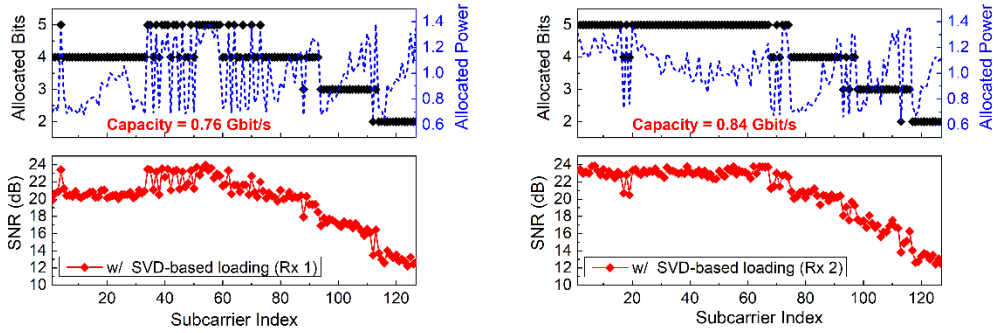

Fig. 7. Allocated bits and power, and the estimated SNR profile by using the SVD-based adaptive loading in scenario 1: Rx 1 (left) and Rx 2 (right). The aggregate data rate is 1.6 Gbit/s.

Figure 7 shows the allocated bits and power as well as the estimated SNR profile in scenario 1. The overall spectral efficiency and the average power are the same as that of the conventional MIMO 16QAM-OFDM in Subsection 4.1: the total bits per symbol at two Txs are $127 \times 4 \times 2 = 1016$ bits; the overall normalized power is $127 \times 2 = 254$ (if we normalize the original power at each data subcarrier as 1). Instead of using the same number of bits and power for all subcarriers, the proposed SVD technique allocates different numbers of bits and power to different Txs as well as different subcarriers within each Tx. The numbers of allocated bits per OFDM symbol are 483 and 533 for the signals transmitted via Tx 1 and Tx 2, resulting in data rates of 0.76 Gbit/s and 0.84 Gbit/s, respectively. The total powers for all subcarriers of the signals at Tx 1 and Tx 2 are 123.3 and 130.7, respectively. It is clear from Fig. 7 that the bit distribution is related to the estimated equivalent CSI, and more bits are assigned to the subcarriers with higher SNR conditions. Accordingly, the power distribution exhibits a saw-tooth behaviour. Compared to the conventional MIMO-OFDM scheme, the

Optics EXPRESS

SVD-based adaptive MIMO-OFDM reduces the BERs of Rx 1 and Rx 2 from 2.35×10^{-3} to 3.31×10^{-6} and from 1.64×10^{-3} to 6.75×10^{-6}, respectively.

Figure 8 shows the allocated bits and power as well as the estimated SNR profile in scenario 2. Similarly, the overall spectral efficiency and average power are the same as that of the conventional MIMO 8QAM-OFDM in Subsection 4.1: the total bits per symbol at two Txs are $127 \times 3 \times 2 = 762$ bits; the overall normalized power is $127 \times 2 = 254$. In contrast to Fig. 7, the allocated numbers of bits for Tx 1 and Tx 2, 429 bits and 333 bits, differ more in the asymmetrical setup, due to higher SNR conditions at Rx 1. The corresponding data rates are 0.68 Gbit/s and 0.52 Gbit/s, wherein the BERs of Rx 1 and Rx 2 are significantly reduced to less than 10^{-6} and 3.60×10^{-6}, respectively.

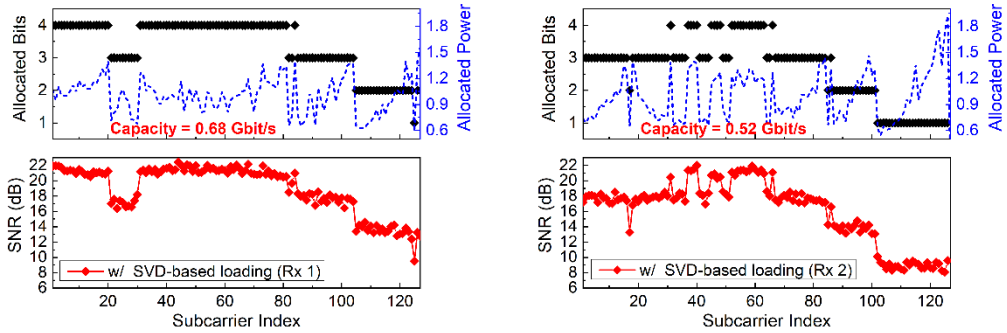

Fig. 8. Allocated bits and power, and the estimated SNR profile by using the SVD-based adaptive loading in scenario 2: Rx 1 (left) and Rx 2 (right). The aggregate data rate is 1.2 Gbit/s.

4.4 Performance comparisons

Finally, we compare the average BER performance of conventional MIMO OFDM, the OCT techniques, and the SVD-based adaptive loading to confirm the performance advantage of the proposed schemes. Figure 9 shows the average BERs versus the length of CP in (a) scenario 1 and (b) scenario 2. The gross data rates of all schemes in the two scenarios are 1.6 Gbit/s and 1.2 Gbit/s, respectively. It is seen that for both scenarios, increasing the length of CP would result in BER reduction, but at the expense of reduced spectral efficiency. When the length of CP is larger than 1/16 of one OFDM symbol, the BER reduction is insignificant. For the symmetrical MIMO setup shown in Fig. 9(a), the BERs of the individual and joint OCT schemes are comparable. In contrast, in scenario 2, the BER performance of the joint OCT technique is better than that of the individual OCT technique. This agrees with the results in Subsection 4.2. For both scenarios, the SVD-based adaptive MIMO-OFDM scheme achieves the optimal performance compared to other schemes.

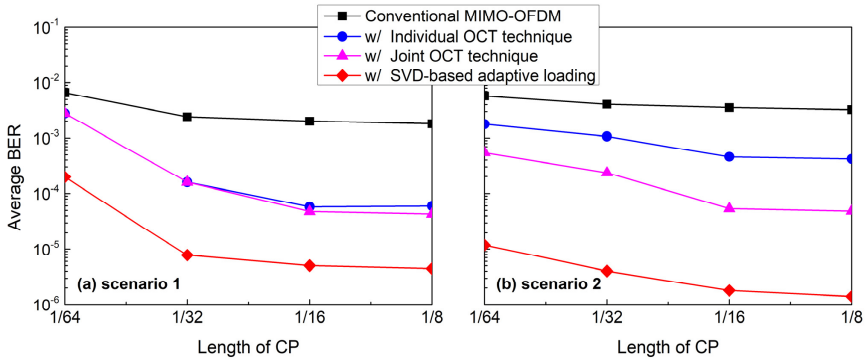

Fig. 9. Average BERs of different schemes versus the length of CP.

Optics EXPRESS

Figure 10 shows the average BERs of different schemes versus the data rate. The length of CP is fixed to 1/16 of one OFDM symbol for all schemes in the two scenarios. For both scenarios, significant BER reductions are achieved by the proposed OCT techniques and SVD-based adaptive loading, when compared to the conventional MIMO-OFDM schemes. As expected, the joint OCT technique exhibits a similar performance improvement as the individual OCT technique in scenario 1, but shows superior performance in scenario 2. Generally, both of the joint OCT technique and the SVD-based adaptive loading can realize joint inter- and intra-subchannel optimization. The difference is that the SVD-based adaptive loading can also realize bits and power re-allocations according to channel properties while the joint OCT technique cannot. Therefore, the SVD-based adaptive MIMO-OFDM scheme attains the best performance in both scenarios. By using the SVD-based adaptive loading, the average BER can be significantly reduced from 1.99×10^{-3} to 5.03×10^{-6} at 1.6 Gbit/s for scenario 1, and from 3.54×10^{-3} to 1.80×10^{-6} at 1.2 Gbit/s for scenario 2. Furthermore, if we take 1×10^{-3} as the BER threshold, the achievable capacity of the overall MIMO-OFDM VLC system can be boosted from ~1.5 Gbit/s to >2.0 Gbit/s and from ~1.1 Gbit/s to >1.5 Gbit/s for scenario 1 and scenario 2, respectively. In contrast, the individual OCT technique only has the capability of intra-subchannel optimization, thus exhibiting less significant BER reduction. Note that as aforementioned, prior knowledge of the CSI is required to implement the SVD-based adaptive MIMO-OFDM scheme, which restricts its application to static setups/channels. On the other hand, the joint OCT technique is more suitable to time-varying systems, since it is CSI-free and shows significant performance improvement regardless of transceivers' geometrical distributions.

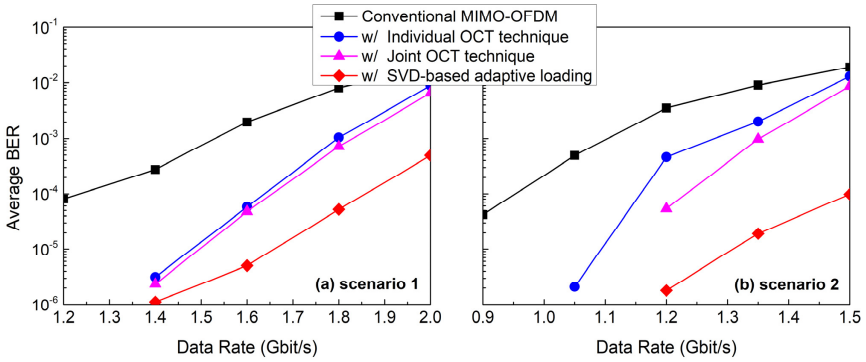

Fig. 10. Average BERs of different schemes versus the data rate.

5. Conclusions

In this paper, we have proposed CSI-free OCT techniques and CSI-dependent SVD-based adaptive loading to improve the performance of bandwidth-limited MIMO-OFDM VLC systems. The proposed schemes are validated in gigabit/s 2 × 2 MIMO-OFDM VLC experiments with ~100-MHz 3-dB system bandwidth, under both symmetrical and asymmetrical MIMO setups. In the 1.6-Gbit/s symmetrical setup, the average BER is reduced from 1.99×10^{-3} to 4.76×10^{-5} and 5.03×10^{-6} by using joint OCT technique and SVD-based adaptive loading, respectively. In the 1.2-Gbit/s asymmetrical MIMO setup, the average BER is reduced from 3.54×10^{-3} to 5.35×10^{-5} and 1.80×10^{-6}, respectively. The results confirm that the joint OCT technique can be a promising CSI-free technique to alleviate the bandwidth limitation issue regardless of geometrical positions of the transceivers, while the SVD-based adaptive loading is the best solution for static MIMO-OFDM VLC systems. This study focuses on the limited bandwidth issue, however the proposed techniques are also applicable to the mitigation of other impairments that result in the frequency-selective response in MIMO-OFDM systems.

Optics EXPRESS

Funding

HKSAR RGC (GRF 14215416, GRF 14201217); China "1000 Youth Talent Program."

References

1. D. Karunatilaka, F. Zafar, V. Kalavally, and R. Parthiban, "LED based indoor visible light communications: state of the art," IEEE Comm. Surv. and Tutor. **17**(3), 1649–1678 (2015).
2. J. Chen, Y. Hong, Z. Wang, and C. Yu, "Precoded visible light communications," in Proceedings of ICICS (IEEE, 2013), 1–4.
3. H. H. Lu, C. Y. Li, C. A. Chu, T. C. Lu, B. R. Chen, C. J. Wu, and D. H. Lin, "10 m/25 Gbps LiFi transmission system based on a two-stage injection-locked 680 nm VCSEL transmitter," Opt. Lett. **40**(19), 4563–4566 (2015).
4. C. Y. Li, H. H. Lu, W. S. Tsai, M. T. Cheng, C. M. Ho, Y. C. Wang, Z. Y. Yang, and D. Y. Chen, "16 Gb/s PAM4 UWOC system based on 488-nm LD with light injection and optoelectronic feedback techniques," Opt. Express **25**(10), 11598–11605 (2017).
5. Y. F. Huang, C. T. Tsai, H. Y. Kao, Y. C. Chi, H. Y. Wang, T. T. Shih, and G. R. Lin, "17.6-Gbps universal filtered multi-carrier encoding of GaN blue LD for visible light communication," in Proceedings of CLEO (IEEE, 2017), STh1C.5.
6. C. Chen, W. Zhong, and D. Wu, "Indoor OFDM visible light communications employing adaptive digital pre-frequency domain equalization," in Procedings of CLEO (IEEE, 2016), JTh2A.118.
7. Y. Hong and L. K. Chen, "Toward user mobility for OFDM-based visible light communications," Opt. Lett. **41**(16), 3763–3766 (2016).
8. R. Deng, J. He, Z. Zhou, J. Shi, M. Hou, and L. Chen, "Experimental demonstration of software-configurable asynchronous real-time OFDM signal transmission in a hybrid fiber-VLLC system," IEEE Photonics J. **9**(1), 7801008 (2017).
9. Y. Hong, J. Xu, and L. K. Chen, "Experimental investigation of multi-band OCT precoding for OFDM-based visible light communications," Opt. Express **25**(11), 12908–12914 (2017).
10. X. Huang, Z. Wang, J. Shi, Y. Wang, and N. Chi, "1.6 Gbit/s phosphorescent white LED based VLC transmission using a cascaded pre-equalization circuit and a differential outputs PIN receiver," Opt. Express **23**(17), 22034–22042 (2015).
11. Y. Hong, J. Chen, and C. Yu, "Performance improvement of the pre-coded multi-user MIMO indoor visible light communication system," in *Proc. of CSNDSP* (*IEEE*, 2014), pp. 314–318.
12. A. Nuwanpriya, S. W. Ho, and C. S. Chen, "Indoor MIMO visible light communications: novel angle diversity receivers for mobile users," IEEE J. Sel. Areas Comm. **33**(9), 1780–1792 (2015).
13. P. M. Butala, H. Elgala, and T. D. C. Little, "SVD-VLC: A novel capacity maximizing VLC MIMO system architecture under illumination constraints," in Proceedings of Globecom (IEEE, 2013), 1087–1092.
14. Y. Hong, T. Wu, and L. K. Chen, "On the performance of adaptive MIMO-OFDM indoor visible light communications," IEEE Photonics Technol. Lett. **28**(8), 907–910 (2016).
15. A. H. Azhar, T. Tran, and D. O'Brien, "A gigabit/s indoor wireless transmission using MIMO-OFDM visible-light communications," IEEE Photonics Technol. Lett. **25**(2), 171–174 (2013).
16. Y. Wang and N. Chi, "Demonstration of high-speed 2 × 2 non-imaging MIMO Nyquist single carrier visible light communication with frequency domain equalization," J. Lightwave Technol. **32**(11), 2087–2093 (2014).
17. C. W. Hsu, C. W. Chow, I. C. Lu, Y. L. Liu, C. H. Yeh, and Y. Liu, "High speed imaging 3 × 3 MIMO phosphor white-light LED based visible light communication system," IEEE Photonics J. **8**(6), 7907406 (2016).
18. Y. Hong, L. K. Chen, and J. Zhao, "Experimental demonstration of performance-enhanced MIMO-OFDM visible light communications," in Proceedings of OFC (Optical Society of America, 2017), Th1E.2.
19. M. Vetterli and H. J. Nussbaumer, "Simple FFT and DCT algorithms with reduced number of operations," Signal Processing **6**(4), 267–278 (1984).
20. S. H. Wang, C. P. Li, K. C. Lee, and H. J. Su, "A novel low-complexity precoded OFDM system with reduced PAPR," IEEE Trans. Signal Process. **63**(6), 1366–1376 (2015).
21. Z. Zhou, B. Vucetic, M. Dohler, and Y. Li, "MIMO systems with adaptive modulation," IEEE Trans. Vehicular Technol. **54**(5), 1828–1842 (2005).
22. P. S. Chow, J. M. Cioffi, and J. A. C. Bingham, "A practical discrete multitone transceiver loading algorithm for data transmission over spectrally shaped channels," IEEE Trans. Commun. **43**(2), 773–775 (1995).